# Effective nonlinear optical properties of metal-dielectric composite media with shape distribution

L. Gao,[1,2] K. W. Yu,[3] Z. Y. Li,[2] and Bambi Hu[1,4]
[1]*Department of Physics and Center for Nonlinear Studies, Hong Kong Baptist University, Hong Kong, China*
[2]*Department of Physics, Suzhou University, Suzhou, 215006, China*
[3]*Department of Physics, The Chinese University of Hong Kong, Shatin New Territories, Hong Kong, China*
[4]*Department of Physics, University of Houston, Houston, Texas 77204*
(Received 20 February 2001; published 29 August 2001)

The effective linear and nonlinear optical properties have been investigated in granular metal-dielectric composites taking the geometric shape of inclusions into account. Recently derived Maxwell-Garnett-type approximations are generalized to study the spectral function for composites in which the metal inclusions have a uniform distribution of geometric shapes. The numerical results show that the spectral density function becomes a prominent peak around small spectral value $s$ within the non-self-consistent Maxwell-Garnett approximation but a broad continuous spectrum around large $s$ besides the prominent peak around small $s$ within the self-consistent Maxwell-Garnett approximation. Based on the spectral representation, we investigate the optical absorption and third-order nonlinear optical susceptibility. The results indicate that the shape distribution can lead to the separation of the nonlinearity enhancement peak from the absorption peak and thereby make the figure of merit more attractive.

DOI: 10.1103/PhysRevE.64.036615 PACS number(s): 42.65.−k, 82.70.Dd, 81.05.Rm, 72.20.Ht

## I. INTRODUCTION

Nonlinear optical properties in random metal-dielectric composite media have been the subject of growing interest in recent years because of their potential applications in physics and engineering [1,2]. A typical system is composed of metal granular particles with a nonlinear dielectric response embedded in a dielectric host with a linear or nonlinear response. It is well known that at frequencies close to the surface plasmon resonances, the third-order nonlinear susceptibility of such a composite system may be greatly enhanced through the local field effects [3–9]. The metal-dielectric composite media are also known to have an anomalously large optical absorption in the infrared region [10]. Both the absorption spectrum and optical nonlinearity are sensitively dependent on the composite microstructure [11–13].

More recently, we derived two different Maxwell-Garnett-type approximations based on whether a self-consistent condition on the net polarization is invoked [14]. The results show that the optical absorption and the third-order nonlinear susceptibility are strongly dependent on the shape of inclusions. However, a large nonlinearity enhancement is always accompanied by a large optical absorption, which hinders practical applications. In this regard, geometric anisotropy [5,15], fractal [7] or correlated microstructure [13] in composites can lead to the separation of the absorption peak from the nonlinearity enhancement peak, resulting in a large figure of merit.

According to the analysis of the absorption coefficient and conjugate reflectivity in related experiments, it has been shown that the granular inclusions may deviate from perfect spherical shape, which possess certain shape distribution [16]. The distribution of granular shapes may also be important in understanding the Lichtenecker's formula [17] and explaining the anomalous far-infrared absorption of small metallic particles [18]. Therefore, in this work, we examine the metal-dielectric system in which metallic inclusions are ellipsoidal in shape, described by some shape distributions. Each ellipsoidal nanoparticle is described by three depolarization factors $L_x$, $L_y$ and $L_z$ (satisfying the sum rule $L_x+L_y+L_z=1$). Generally, the granular inclusions are randomly oriented and the effective response is still isotropic. We will generalize the Maxwell-Garnett-type approximations [14] in conjunction with the spectral representation [19–21] to investigate both the linear and nonlinear optical properties of such composite media.

We organize the paper as follows. In the next two sections, we derive the two Maxwell-Garnett-type approximations by taking the shape distribution of inclusions into account, and then calculate the spectral density function numerically. With the spectral density, we study the optical absorption and the enhancement of third-order nonlinear susceptibility in Sec. IV. A summary of our results and discussions will be given in Sec. V.

## II. NON-SELF-CONSISTENT MAXWELL-GARNETT APPROXIMATION (MGA1)

Let us consider a nonlinear granular composite in which randomly oriented, ellipsoidal metal particles of volume fraction $f$ are embedded in an isotropic dielectric host of volume fraction $1-f$. We assume that the particle size is much smaller than the wavelength of light so that the quasistatic approximation can be adopted. The local constitutive electric displacement ($\mathbf{D}$)-electric field ($\mathbf{E}$) relation is given by $\mathbf{D}=\epsilon_i^{(0)}\mathbf{E}+\chi_i^{(3)}|\mathbf{E}|^2\mathbf{E}$, where $\epsilon_i^{(0)}$ and $\chi_i^{(3)}$ are the (scalar) linear dielectric function and the third-order nonlinear optical susceptibility of the $i$th component ($i=1,2$). The nonlinear term of the component is always assumed to be weak in comparison with the linear one [3,5,6,11–15]. Since the axes of the ellipsoidal particles are randomly distributed in space (corresponding to a uniform distribution of ellipsoidal inclusions over the entire solid angles), the effective response is

 

still isotropic. Ellipsoidal particles are described by three depolarization factors $L_x$, $L_y$, and $L_z$, which satisfy the sum rule $L_x+L_y+L_z=1$. For spherical particles $L_x=L_y=L_z=1/3$, while for cylindrical ones, $L_z=0$ and $L_x=L_y=1/2$. In general, the coefficient $L_j(j=x,y,z)$ is shape dependent and has the form [22]

$$L_j=\frac{a_x a_y a_z}{2}\int_0^\infty \frac{du}{(a_j^2+u)\sqrt{(a_x^2+u)(a_y^2+u)(a_z^2+u)}}, \quad (1)$$

where $a_x$, $a_y$, and $a_z$ are semi axes of the inclusion parallel to the three Cartesian coordinate axes $x$, $y$, and $z$. With given $a_j(j=x,y,z)$, one can determine uniquely a depolarization $L_j$. Thus we may use the depolarization factor to characterize the shape of the ellipsoidal particles. A prescribed distribution of the depolarization factor will be adopted to describe the distribution of the geometric shapes of the inclusions.

The average electric field $\langle \mathbf{E}_1 \rangle$ in the ellipsoidal inclusions is given by [3,14]

$$\langle \mathbf{E}_1 \rangle = \frac{1}{3}\sum_{j=x}^{z} \frac{\epsilon_2^{(0)}}{L_j\epsilon_1^{(0)}+(1-L_j)\epsilon_2^{(0)}}\langle \mathbf{E}_L \rangle, \quad (2)$$

where $\langle \mathbf{E}_L \rangle$ is the Lorentz local field.

The expression for the spatial average of the electric field over the whole volume of composite is

$$\langle \mathbf{E} \rangle = f\langle \mathbf{E}_1 \rangle + (1-f)\langle \mathbf{E}_L \rangle. \quad (3)$$

Similarly, the bulk average of the dielectric displacement $\langle \mathbf{D} \rangle$ is

$$\langle \mathbf{D} \rangle = f\epsilon_1^{(0)}\langle \mathbf{E}_1 \rangle + (1-f)\epsilon_2^{(0)}\langle \mathbf{E}_L \rangle. \quad (4)$$

The effective linear dielectric function $\epsilon_e^{(0)}$ can be defined as

$$\epsilon_e^{(0)} = \frac{\langle \mathbf{D} \rangle}{\langle \mathbf{E} \rangle} = \frac{f\epsilon_1^{(0)}\beta + (1-f)\epsilon_2^{(0)}}{f\beta + 1 - f}, \quad (5)$$

where $\beta \equiv \langle \mathbf{E_1} \rangle / \langle \mathbf{E_L} \rangle = \frac{1}{3}\Sigma_j \epsilon_2^{(0)}/[L_j\epsilon_1^{(0)}+(1-L_j)\epsilon_2^{(0)}]$ is the field factor.

In order to investigate the effect of a shape distribution of granular inclusions on the effective linear and nonlinear optical properties, we propose a distribution function $P(L_x,L_y,L_z)$ of depolarizations factors to characterize the shape distribution. The distribution function $P(L_x,L_y,L_z)$ must be chosen to satisfy $\int\int_\sigma P(L_x,L_y,L_z)d\sigma=1$, where $\sigma$ is the area of the plane, $L_x+L_y+L_z=1$. Correspondingly, the field factor should be obtained from

$$\langle \beta \rangle_{shdis} = \frac{1}{3}\int\int_\sigma P(L_x,L_y,L_z)\sum_j \frac{\epsilon_2^{(0)}}{L_j\epsilon_1^{(0)}+(1-L_j)\epsilon_2^{(0)}}d\sigma. \quad (6)$$

For convenience, we assume that the shape of inclusions distributes uniformly and $P(L_x,L_y,L_z)=2/\sqrt{3}$ by exhausting all possible ellipsoids. Alternative distribution such as the binary distribution [23], $\Gamma$ distribution [17], and log-normal distribution [23] can be treated similarly. The expression for the field factor with a uniform distribution of depolarization factors can be simplified as

$$\beta = \frac{2}{\left(1-\frac{\epsilon_1^{(0)}}{\epsilon_2^{(0)}}\right)^2}\left[1-\frac{\epsilon_1^{(0)}}{\epsilon_2^{(0)}}+\frac{\epsilon_1^{(0)}}{\epsilon_2^{(0)}}\ln\left(\frac{\epsilon_1^{(0)}}{\epsilon_2^{(0)}}\right)\right]. \quad (7)$$

The effective linear dielectric function of composites with a uniform shape distribution can be obtained by substituting Eq. (7) into Eq. (5).

In the dilute limit, i.e., $f\to 0$, Eq. (7) reduces to

$$\epsilon_e^{(0)} = \epsilon_2^{(0)}\left[1+2f\left(\frac{\epsilon_1^{(0)}}{\epsilon_1^{(0)}-\epsilon_2^{(0)}}\ln\frac{\epsilon_1^{(0)}}{\epsilon_2^{(0)}}-1\right)\right], \quad (8)$$

which was first derived in Ref. [18].

As claimed in Refs. [14] and [24], because the mutual interaction between different polarizations is neglected, as in the case of small volume fractions, Eq. (5) with Eq. (7) may be valid for not too large volume fractions such as $f\leqslant 0.3$. At large volume fractions $f>0.3$, the interactions between particles must be considered.

Then we calculate the spectral density function. For two-component composites, it has proved convenient to adopt the spectral representation of effective linear response [19–21]. Let $s=\epsilon_2^{(0)}/(\epsilon_2^{(0)}-\epsilon_1^{(0)})$ and $F=1-\epsilon_e^{(0)}/\epsilon_2^{(0)}$, we find

$$F(s)=\int_0^1 \frac{m(s')}{s-s'}ds', \quad (9)$$

where $m(s')$ is the spectral density function, which can be obtained through the limiting process,

$$m(s') = \lim_{\eta\to 0^+} -\frac{1}{\pi}\mathrm{Im}[F(s'+i\eta)]. \quad (10)$$

While the analytic solution for the spectral density function may exist, here we resort to numerical calculation. We calculate $m(s')$ numerically from Eqs. (5) and (7)–(10). We put $s=s'+i\eta$ and choose the real part at 1,000 equally spaced across the interval value $0<s'<1$ and $\eta$ at some positive values such as $\eta=0.001$. The actual value of $\eta$ is indeed unimportant. We find that such choice gives acceptable results by checking the sum rule

$$\int_0^1 m(s')ds' = f. \quad (11)$$

In Fig. 1, we plot the spectral density $m(s)$ against $s$ for various volume fractions $f=0.05$, 0.1, and 0.3. When we take into account the shape distribution, the spectrum turns broad and has a large spectral peak around small $s$. This is due to the fact that in the composite system with the shape distribution, the larger clusters are more easily enhanced at the expense of smaller ones than they are in the standard Maxwell-Garnett model. The large values of spectral peak in

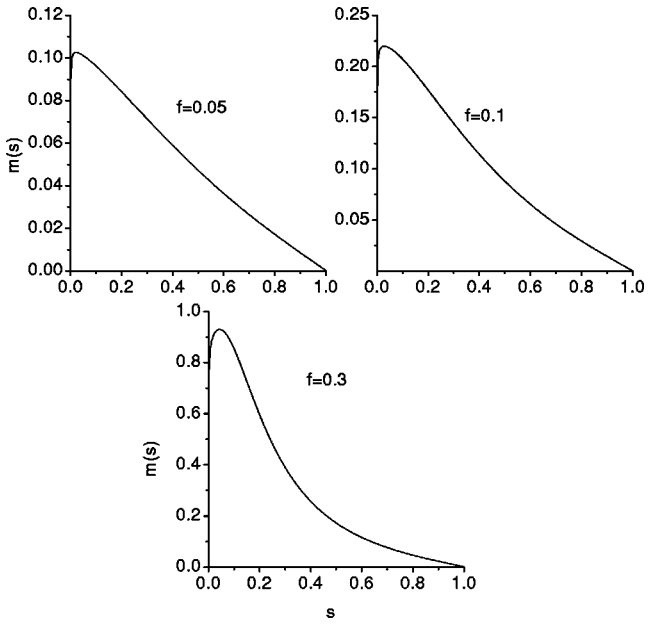


FIG. 1. The spectral density $m(s)$ within MGA1 against $s$ for various $f=0.05$, 0.1, and 0.3.

the small-$s$ range will be useful to increase the optical absorption in the infrared region. The results indicate that the shape distribution of metal particles plays a role in explaining the anomalous far-infrared absorption. The spectra increase in small-$s$ region and reach maximum values and then decrease in large-$s$ region. Moreover, they are continuous in the whole range from $s=0$ to $s=1$, in contrast to two $\delta$-type sharp peaks in composites of spheroidal particles with same depolarization factors [14]. When increasing the volume fraction $f$, the location of the spectral peak are almost invariant, but the magnitude of the peak becomes large so as to satisfy the sum rule Eq. (11).

### III. SELF-CONSISTENT MAXWELL-GARNETT TYPE APPROXIMATION (MGA2)

We generalize the cellular model [14,25] to study the system in which the ellipsoidal metal inclusions are dispersed in a dielectric host. To formulate the cellular model, we construct the Wigner-Seitz cell of each microellipsoid and replace the composite by a fictitious homogeneous medium of an as-yet undetermined dielectric constant $\epsilon_m^{(0)}$, except for one of the cells. The cell is then replaced by an ellipsoidal core of dielectric constant $\epsilon_1^{(0)}$, coated by a confocal shell of $\epsilon_2^{(0)}$. The core and the shell have the same aspect ratio, characterized by $r=a_{cx}/a_{sx}=a_{cy}/a_{sy}=a_{cz}/a_{sz}$, where the subscript $c$ and $s$ mean core and shell.

The effective linear dielectric constant $\epsilon_e^{(0)}$ is given by the dilute-limit expression,

$$\epsilon_e^{(0)}=\epsilon_m^{(0)}+p\epsilon_m^{(0)}[b_x(\epsilon_1^{(0)},\epsilon_2^{(0)},\epsilon_m^{(0)},y)+b_y(\epsilon_1^{(0)},\epsilon_2^{(0)},\epsilon_m^{(0)},y)+b_z(\epsilon_1^{(0)},\epsilon_2^{(0)},\epsilon_m^{(0)},y)], \tag{12}$$

where $p$ is an infinitesimal volume fraction and $y\equiv(a_{cx}a_{cy}a_{cz})/(a_{sx}a_{sy}a_{sz})$ is the volume ratio of the core to the whole coated ellipsoid, and $b_j$ is the dipole factor to a single-coated ellipsoidal inclusion along the $j$ axis,

$$b_j=\frac{1}{3}\frac{(\epsilon_2^{(0)}-\epsilon_m^{(0)})[\epsilon_2^{(0)}+L_j(\epsilon_1^{(0)}-\epsilon_2^{(0)})]+(\epsilon_1^{(0)}-\epsilon_2^{(0)})y[\epsilon_2^{(0)}+L_j(\epsilon_m^{(0)}-\epsilon_2^{(0)})]}{(\epsilon_2^{(0)}-\epsilon_1^{(0)})(\epsilon_m^{(0)}-\epsilon_2^{(0)})yL_j(1-L_j)+[\epsilon_2^{(0)}+(\epsilon_1^{(0)}-\epsilon_2^{(0)})L_j][\epsilon_m^{(0)}+(\epsilon_2^{(0)}-\epsilon_m^{(0)})L_j]}. \tag{13}$$

The effective dielectric constant $\epsilon_e^{(0)}$ can be obtained self-consistently with Eqs. (12) and (13), if we identify $y$ with $f$ and $\epsilon_m^{(0)}$ with $\epsilon_e^{(0)}$; then Eq. (12) becomes a self-consistency equation, which readily implies that,

$$b=b_x+b_y+b_z=0 \quad \text{or} \quad \sum_x^z b_j=0. \tag{14}$$

Here we would like to point out that the mutual interaction between different polarizations is taken into account in a self-consistent way and Eq. (14) can thus be used for large volume fractions [14]. When the microellipsoid becomes microsphere, our theoretical model is nothing but the Hashin-Shtrikman one, in which the volume fraction of the component can vary from 0 to 1.0 [26].

We then introduce a prescribed type of distribution for the depolarization factors $P(L_x,L_y,L_z)$, the self-consistency equation becomes

$$\langle b\rangle_{shdis}=\int\int_\sigma P(L_x,L_y,L_z)(b_x+b_y+b_z)d\sigma=0. \tag{15}$$

Again, $P(L_x,L_y,L_z)$ must be chosen to satisfy $\langle 1\rangle_{shdis}=1$ and for uniform one $P(L_x,L_y,L_z)=2/\sqrt{3}$.

We plot $m(s)$ versus $s$ for small volume fractions such as $f=0.05$ and $f=0.1$ in Fig. 2(a) and large volume fractions $f=0.3$, 0.5, and 0.7 in Fig. 2(b) within MGA2. For small volume fractions, say $f=0.05$ and $f=0.1$, a spectral peak around small $s$ arises as expected. As we include the mutual interaction between different polarizations into calculations, the dominant peak [see Fig. 2(a)] broadens in comparison with that shown in Fig. 1. However, for large volume fractions $f=0.3$, 0.5, and 0.7, it is seen from Fig. 2(b) that there is a broad continuous spectrum band in large-$s$ region, in addition to a prominent broad band in small-$s$ region. Such behavior is quite different from that predicted within MGA1.

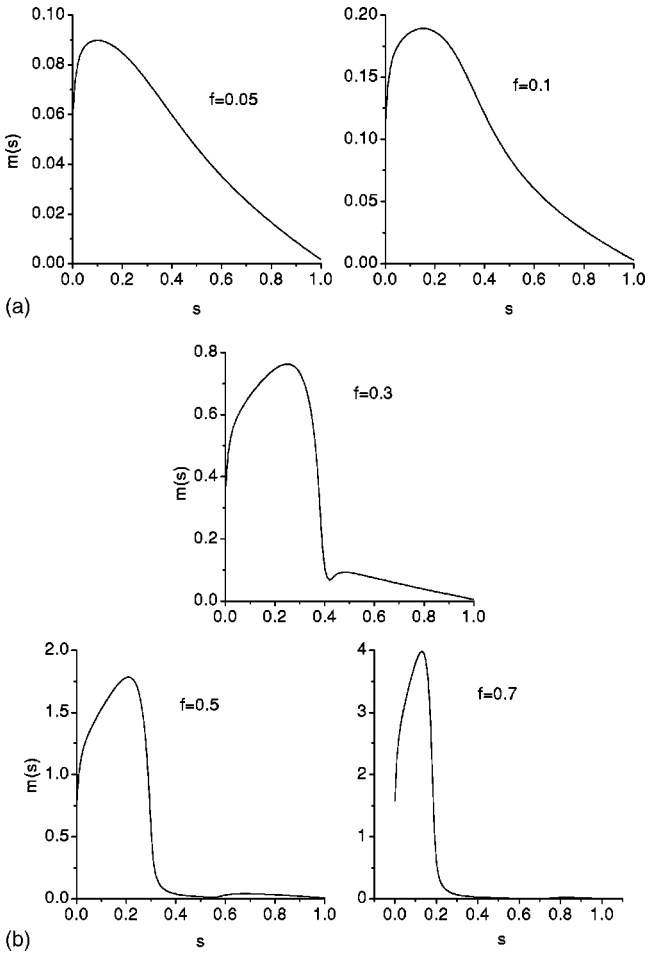


FIG. 2. $m(s)$ within MGA2 against $s$ for small volume fractions $f=0.05$ and 0.1 (a) and large volume fractions $f=0.3$, 0.5, and 0.7 (b).

We believe that the mutual interaction between different polarizations contributes to this broad continuous spectrum, and the shape distribution enhances the magnitude of the spectral density further. When $f$ gradually increases, interaction among granular inclusions becomes strong, resulting in a broad spectral band in the small-$s$ region. However, with further increase of $f$, metal clusters get collected, leading to the narrow spectrum.

## IV. THE OPTICAL ABSORPTION AND THIRD-ORDER NONLINEAR SUSCEPTIBILITY

As we have obtained the spectral density by means of two approximations, we can next examine the effective linear dielectric constant with the following equation

$$\epsilon_e^{(0)}=\epsilon_2^{(0)}\left[1-\int_0^1\frac{m(s')}{s-s'}ds'\right], \tag{16}$$

and effective third-order nonlinear optical susceptibility with [5,11]

$$\chi_e^{(3)}|\mathbf{E_0}|^2\mathbf{E_0}^2=f\chi_1^{(3)}\langle|\mathbf{E}|^2\mathbf{E}^2\rangle_{lin,1}+(1-f)\chi_2^{(3)}\langle|\mathbf{E}|^2\mathbf{E}^2\rangle_{lin,2}$$
$$\approx f\chi_1^{(3)}\langle|\mathbf{E}|^2\rangle_{lin,1}\langle\mathbf{E}^2\rangle_{lin,1}+(1-f)\chi_2^{(3)}$$
$$\times\langle|\mathbf{E}|^2\rangle_{lin,2}\langle\mathbf{E}^2\rangle_{lin,2}, \tag{17}$$

where the linear local field averages $\langle\mathbf{E}^2\rangle_{lin,i}$ and $\langle|\mathbf{E}|^2\rangle_{lin,i}$ are given by

$$f\langle\mathbf{E}^2\rangle_{lin,1}=\int_0^1\frac{s^2m(s')}{(s-s')^2}ds'\mathbf{E_0}^2,$$

$$(1-f)\langle\mathbf{E}^2\rangle_{lin,2}=\left[1-\int_0^1\frac{(s^2-s')m(s')}{(s-s')^2}ds'\right]\mathbf{E_0}^2, \tag{18}$$

and

$$f\langle|\mathbf{E}|^2\rangle_{lin,1}=\int_0^1\frac{|s|^2m(s')}{|s-s'|^2}ds'|\mathbf{E_0}|^2,$$

$$(1-f)\langle|\mathbf{E}|^2\rangle_{lin,2}=\left[1-\int_0^1\frac{(|s|^2-s')m(s')}{|s-s'|^2}ds'\right]|\mathbf{E_0}|^2. \tag{19}$$

The mean field approximation is adopted in Eq. (17), which holds well when the field inside the component $i$ is a constant.

As numerical illustration, we adopt the Drude free-electron model for the dielectric function of metal particles

$$\epsilon_1^{(0)}(\omega)=1-\frac{\omega_p^2}{\omega(\omega+i\gamma)}, \tag{20}$$

where $\omega_p$ denotes the plasmon frequency and $\gamma$ is the damping constant. We choose $\gamma=0.01\omega_p$, which is typical of a good bulk metal and $\epsilon_2^{(0)}=1.77$ is the dielectric constant of water. We assume the dielectric host to be linear, i.e., $\chi_2^{(3)}=0$, based on the fact that the optical nonlinearity of dielectric host is several orders of magnitude smaller than that of metal particles and the contribution of the dielectric host to the effective nonlinearity is small [29].

In Fig. 3(a), we show that the optical absorption $\mathrm{Im}(\epsilon_e^{(0)})$ versus frequency $\omega/\omega_p$ for various $f$ within MGA1. Similar to the spectral function shown in Fig. 1, there is a large absorption peak at the surface plasmon resonance frequency (SPRF) for each volume fraction. Large optical absorption has been clearly observed in the far-infrared region especially for small volume fractions such as $f=0.05$. This phenomenon differs from our previous prediction in Ref. [14], as the shape distribution is not included into calculations. With increasing $f$, the resonant absorption peak shifts slightly towards a short wavelength and then a long wavelength by a sharpening of the absorption peak due to the size increase of the metal clusters. This prediction is consistent with the experimental phenomena [30,31].

Then, we concentrate on the enhancement of optical nonlinearity $|\chi_e^{(3)}|/\chi_1^{(3)}$, as shown in Fig. 3(b) within MGA1. $|\chi_e^{(3)}|/\chi_1^{(3)}$ is found to be enhanced in most of the frequency

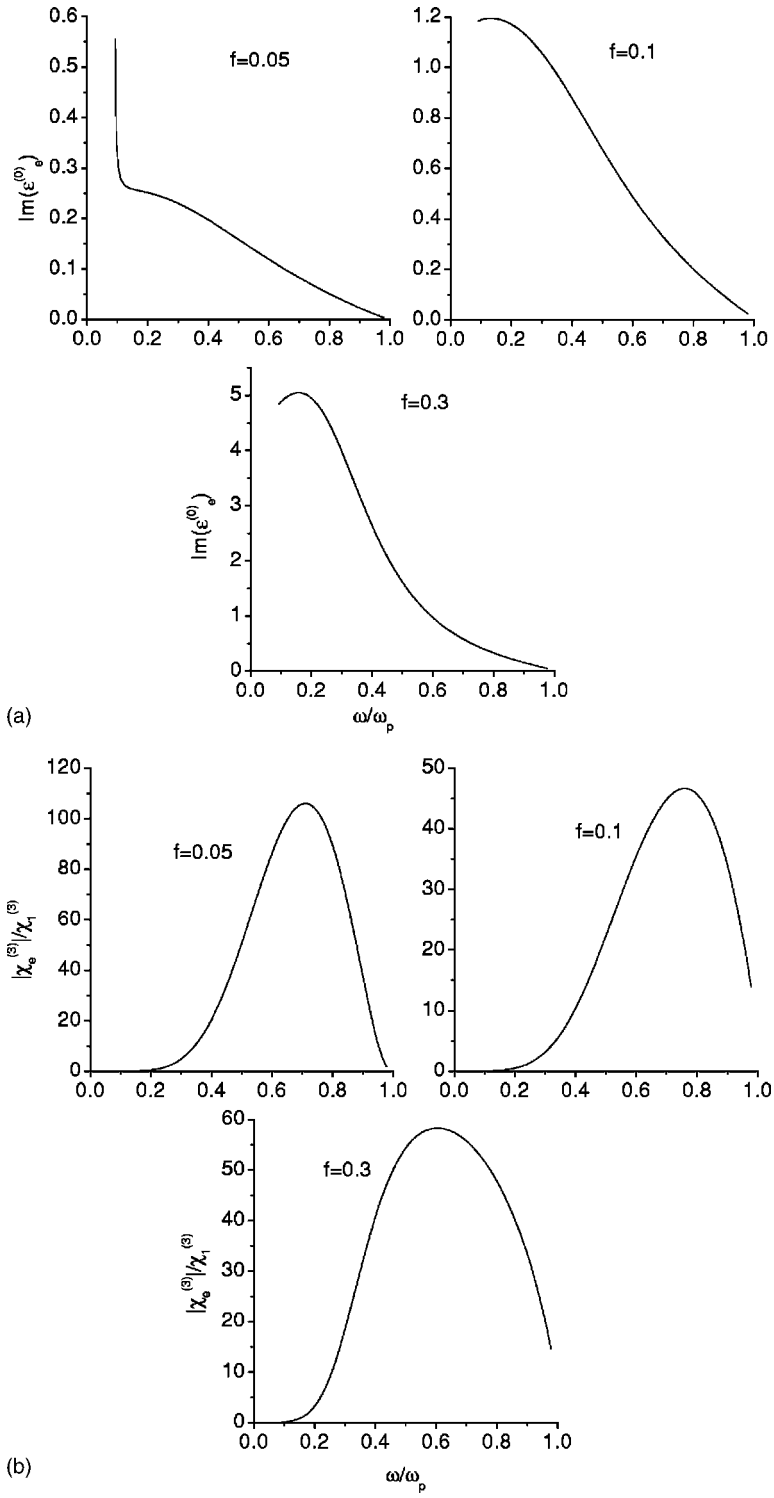


FIG. 3. The optical absorption $\mathrm{Im}(\epsilon_e^{(0)})$ (a) and the enhancement of optical nonlinearity $|\chi_e^{(3)}|/\chi_1^{(3)}$ (b) against the frequency $\omega/\omega_p$ for $f=0.05$, 0.1, and 0.3 within MGA1.

region $0<\omega/\omega_p<1$ and takes a maximum value at certain frequency, which is not equal to the SPRF. The magnitude of nonlinearity enhancement is two orders smaller than previous theoretical prediction [11], but can be comparable with experimental reports [30,31]. With the increase of $f$, on the one hand, the nonlinearity enhancement peak exhibits a blue shift and then a red shift; on the other hand, the nonlinearity enhancement band turns broad as interactions among clusters become strong. More interestingly, the nonlinearity enhancement peak does not coincide with the absorption peak and the separation of the absorption peak from the $\chi_e^{(3)}$ enhancement peak is clearly observed. Therefore it is possible to obtain more prominent optical nonlinearity with a concomitant small linear optical absorption at the frequency of inci-

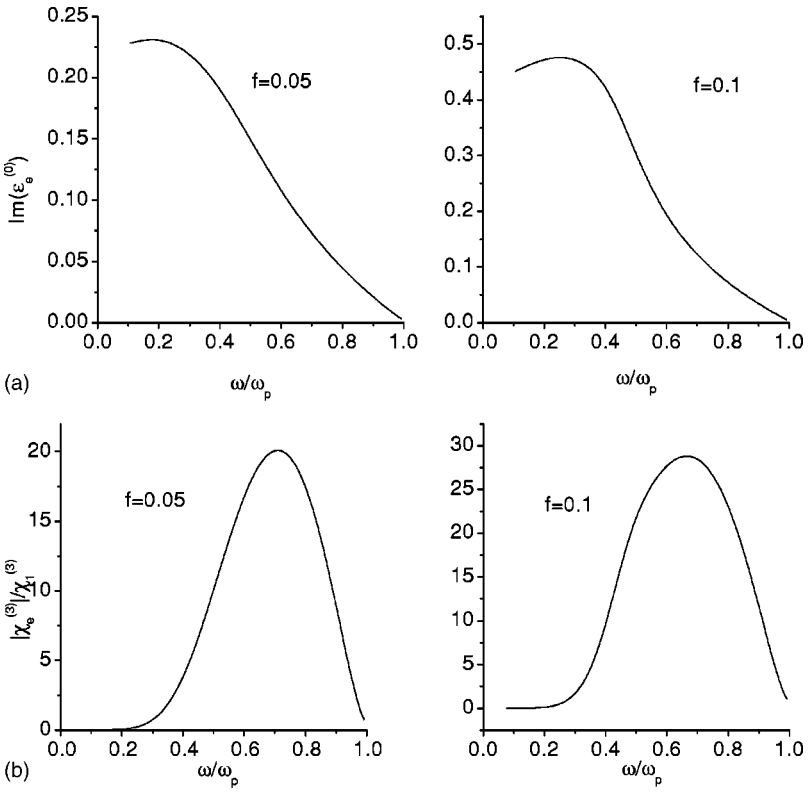


FIG. 4. Similar to Fig. 3 but within MGA2 for small volume fractions $f=0.05$ and 0.1.

dent light far from the SPRF, at which the optical absorption achieves a maximum value. For practical applications, the more useful parameter is the figure of merit, which is proportional to $|\chi_e^{(3)}|$ but inversely proportional to $\mathrm{Im}(\epsilon_e^{(0)})$. Thus a large $|\chi_e^{(3)}|$ is insufficient unless $|\chi_e^{(3)}|/\mathrm{Im}(\epsilon_e^{(0)})$ can be made as large as possible. Most of theoretical works predict that the increase of optical nonlinearity is always accompanied by an increase in light absorption. This reduces the applicability of optical nonlinearity of composites. Here we demonstrate that both $|\chi_e^{(3)}|$ and $|\chi_e^{(3)}|/\mathrm{Im}(\epsilon_e^{(0)})$ can be greatly enhanced in certain frequency region. For example, $|\chi_e^{(3)}|/\mathrm{Im}(\epsilon_e^{(0)}) \sim 1530\chi_1^{(3)}$esu cm for $f=0.05$ at $\omega \approx 0.7\omega_p$ and $|\chi_e^{(3)}|/\mathrm{Im}(\epsilon_e^{(0)}) \sim 200\chi_1^{(3)}$esu cm for $f=0.1$ at $\omega \approx 0.76\omega_p$.

We plot the linear optical absorption $\mathrm{Im}(\epsilon_e^{(0)})$ and $|\chi_e^{(3)}|/\chi_1^{(3)}$ versus $\omega/\omega_p$ for small volume fractions $f=0.05$ and 0.1 in Fig. 4 and large volume fractions $f=0.3$, 0.5, and 0.7 in Fig. 5 within MGA2.

For small volume fractions, as is evident from Fig. 4(a), the optical absorption exhibits similar behavior as that observed in the case of MGA1 [see Fig. 3(a)], especially for $f=0.1$. However, two approximations yield distinct results for large volume fractions. In Fig. 5(a), we find that in the frequency band $0<\omega<0.5\omega_p$, there is a surface plasmon resonance band, which is broader than that obtained within MGA1; while in the large frequency band region such as $\omega > 0.5\omega_p$, a broad continuous absorption spectrum with small magnitude is predicted as a result of mutual interaction between different polarizations, which is absent within MGA1.

In the end, we examine the optical nonlinearity enhancement $|\chi_e^{(3)}|/\chi_1^{(3)}$ within MGA2. for small volume fractions, such as $f=0.05$ and 0.1 [see Fig. 4(b)], appreciable nonlinearity enhancement has been observed in high-frequency region, which is again far from SPRF, so that the figure of merit $|\chi_e^{(3)}|/\mathrm{Im}(\epsilon_e^{(0)})$ can be greatly enhanced. Introducing shape distribution in this frequency region can lead to large enhancement of optical nonlinearity and figure of merit, and is thus beneficial for practical applications. For instance, for $f=0.05$ and 0.1, we attain $|\chi_e^{(3)}|/\mathrm{Im}(\epsilon_e^{(0)}) \sim 285\chi_1^{(3)}$esu cm and $\sim 300\chi_1^{(3)}$esu cm at $\omega \approx 0.7\omega_p$, respectively. For large volume fractions [see Fig. 5(b)], sharp enhancement of optical nonlinearity is seen at low frequencies near the edge of surface plasmon resonance band, especially just above the upper edge of the large linear optical absorption band. In the large frequency region $0.6\omega_p<\omega<1.0\omega_p$, continuous broad band of nonlinearity enhancement is also observed, in analogy to the behavior of linear absorption, shown in Fig. 5(a). We also find that, as $f$ increases, the resonant low frequency and the center of the nonlinearity enhancement band are red shifted and blue shifted respectively.

## V. DISCUSSIONS AND CONCLUSIONS

In this work, we have studied the effect of the shape distribution of inclusions on the optical absorption and the enhancement of optical nonlinearity of metal-dielectric composites. Previously derived Maxwell-Garnett approximations are generalized to investigate the spectral density function of such system. The results show that introducing the shape distribution is helpful to explain qualitatively the large optical absorption and to reduce the discrepancy between theoretical and experimental results on the optical nonlinearity enhancement. More interestingly, at certain frequency region, the uniform shape distribution can lead to the suppres-

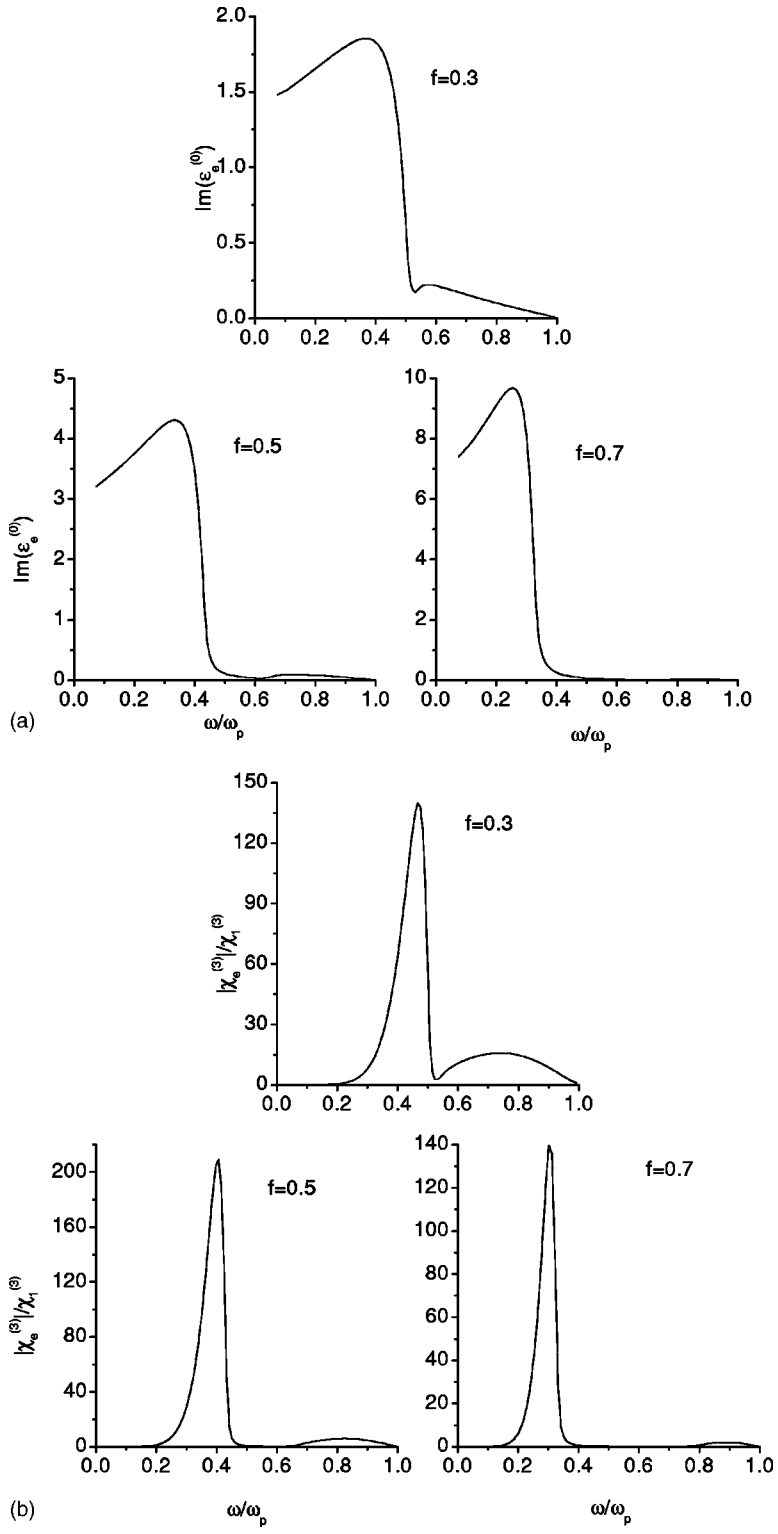


FIG. 5. Similar to Fig. 3 but within MGA2 for large volume fractions $f=0.3$, 0.5, and 0.7.

sion of optical absorption and the concomitant enhancement of optical nonlinearity, and thereby increase the figure of merit.

Here we should add a few comments regarding our results. We can further extend our methods to the system in which both metal particles and the dielectric matrix are nonlinear. We only introduce simple shape distribution function, i.e., uniform shape distribution, into our calculations, other more realistic and complicated distribution function should be chosen to satisfy the experimental case. We consider the Maxwell-Garnett-type models (i.e., distinct inclusion particles are embedded in a dielectric host). For percolation composites, we should adopt the Bruggeman-type effective medium approximation [27,28] by taking the shape distribu-

tion into account.

We may manipulate composite microstructure, such as by the use of correlated, fractal, and anisotropic microstructure to achieve a large enhancement of optical nonlinearity and a concomitant suppression of linear absorption. In this paper, we present another way to realize the separation of linear absorption peak from the nonlinearity enhancement peak by the introduction of the shape distribution of granular inclusions. Our calculation may be qualitatively relevant to recent optical nonlinearity enhancement experiments on metal-dielectric nanocomposites [30–32], in which large third-order optical nonlinearity was studied at the SPRF. In order to compare with experimental results quantitatively, we should apply the Shalaev-Sarychev theory [7,9], describing the interaction effects. We predict that in order to further promote optical nonlinearity and the figure of merit, granular inclusions with certain shape distributions should be prepared and the composite may not be studied at the SPRF, at which the optical absorption achieves a maximum value. We hope our theoretical prediction can stimulate experimental investigations or numerical simulations on this topic.

## ACKNOWLEDGMENTS

This project is supported in part by grants from the Hong Kong Research Grants Council (RGC) and the Hong Kong Baptist University Faculty Research Grant (FRG). Z.Y.L. acknowledges the National Natural Science Foundation of China for financial support under Grant No. 19774042. K.W.Y. acknowledges the Research Grant Council of Hong Kong SAR government under Project No. CUHK 4290/98P.

[1] C. Flytzanis, F. Hache, M. C. Klein, D. Ricard, and P. Roussignol, Prog. Opt. **29**, 323 (1991).
[2] See J. Opt. Soc. Am. B **6** (1989), special issue on nonlinear optical properties of materials, edited by C. M. Bowden and J. W. Haus.
[3] D. Stroud and V. E. Wood, J. Opt. Soc. Am. B **6**, 778 (1989).
[4] C. Flytzanis, Prog. Opt. **29**, 2539 (1992).
[5] K. P. Yuen, M. F. Law, K. W. Yu, and P. Sheng, Phys. Rev. E **56**, R1322 (1997).
[6] L. Gao and Z. Y. Li, J. Appl. Phys. **87**, 1620 (2000).
[7] V. M. Shalaev, *Nonlinear Optics of Random Media: Fractal Composites and Metal-Dielectric Films* (Springer-Verlag, Berlin, 2000). For fractal composites, large magnitude of the figure of merit has been predicted due to the separation of the optical nonlinearity peak from the absorption peak.
[8] V. A. Shubin, A. K. Sarychev, J. P. Clerc, and V. M. Shalaev, Phys. Rev. B **62**, 11 230 (2000).
[9] A. K. Sarychev and V. M. Shalaev, Phys. Rep. **335**, 275 (2000), and references cited therein.
[10] D. B. Tanner, A. J. Sievers, and R. A. Buhrman, Phys. Rev. B **11**, 1330 (1975).
[11] H. R. Ma, R. F. Xiao, and P. Sheng, J. Opt. Soc. Am. B **15**, 1022 (1998).
[12] Y. M. Wu, L. Gao, and Z. Y. Li, Phys. Status Solidi B **220**, 997 (2000).
[13] M. F. Law, Y. Gu, and K. W. Yu, Phys. Rev. B **58**, 12 536 (1998).
[14] L. Gao, J. T. K. Wan, K. W. Yu, and Z. Y. Li, J. Phys.: Condens. Matter **12**, 6825 (2000).
[15] K. P. Yuen, M. F. Law, K. W. Yu, and P. Sheng, Opt. Commun. **148**, 197 (1998).
[16] A. Heilmann, M. Quinten, and J. Werner, Eur. Phys. J. B **3**, 455 (1998).
[17] T. Zakri, J. P. Laurent, and M. Vauclin, J. Phys. D **31**, 1589 (1998).
[18] X. H. Cao, Can. J. Phys. **78**, 113 (2000).
[19] R. Fuchs, Phys. Rev. B **11**, 1732 (1975).
[20] D. J. Bergman, Phys. Rep. **43**, 377 (1978).
[21] G. W. Milton, J. Appl. Phys. **52**, 5286 (1981).
[22] L. D. Landau and E. M. Lifshitz, *Electrodynamics of Continuous Media* (Pergamon, Oxford, 1960).
[23] L. Gao, J. T. K. Wan, Z. Y. Li, and K. W. Yu, J. Appl. Phys. **88**, 1893 (2000).
[24] C. W. Nan, R. Birringer, D. R. Clarke, and H. Gleiter, J. Appl. Phys. **81**, 6692 (1997).
[25] K. W. Yu, Jones, T. K. Wan, M. F. Law, and K. K. Leung, Int. J. Mod. Phys. C **9**, 1447 (1998).
[26] Z. Hashin and S. Shtrikman, J. Appl. Phys. **33**, 3125 (1962).
[27] T. W. Noh, P. H. Song, and A. J. Sievers, Phys. Rev. B **44**, 5459 (1991).
[28] A. N. Lagarkov and A. K. Sarychev, Phys. Rev. B **53**, 6318 (1996).
[29] H. B. Liao, R. F. Xiao, J. S. Fu, and G. K. Wong, Appl. Phys. B: Lasers Opt. **65**, 673 (1997).
[30] H. B. Liao, R. F. Xiao, J. S. Fu, P. Yu, G. K. L. Wong, and P. Sheng, Appl. Phys. Lett. **70**, 1 (1997).
[31] H. B. Liao, R. F. Xiao, H. Wang, K. S. Wong, and G. K. L. Wong, Appl. Phys. Lett. **72**, 1817 (1998).
[32] S. Debrus, J. Lafait, M. May, N. Pincon, D. Prot, C. Sella, and J. Venturini, J. Appl. Phys. **88**, 4469 (2000).